Available online at www.sciencedirect.com
ScienceDirect
Phytochemistry 69 (2008) 663–671
PHYTOCHEMISTRY
www.elsevier.com/locate/phytochem

ESP and *ESM1* mediate indol-3-acetonitrile production from indol-3-ylmethyl glucosinolate in Arabidopsis

Meike Burow [a,c], Zhi-Yong Zhang [b], James A. Ober [b], Virginia M. Lambrix [b], Ute Wittstock [c], Jonathan Gershenzon [a], Daniel J. Kliebenstein [b,*]

[a] *Max-Planck-Institute for Chemical Ecology, Hans-Knöll-Strasse 8, D-07745 Jena, Germany*
[b] *Department of Plant Sciences, Mail Stop 3, University of California, One Shields Avenue, Davis, CA 95616, USA*
[c] *Institut für Pharmazeutische Biologie, Technische Universität Braunschweig, Mendelssohnstr. 1, D-38106 Braunschweig, Germany*

Received 8 May 2007; received in revised form 1 August 2007
Available online 24 October 2007

Abstract

Glucosinolates are plant secondary metabolites that act as direct defenses against insect herbivores and various pathogens. Recent analysis has shown that methionine-derived glucosinolates are hydrolyzed/activated into either nitriles or isothiocyanates depending upon the plants genotype at multiple loci. While it has been hypothesized that tryptophan-derived glucosinolates can be a source of indole-acetonitriles, it has not been explicitly shown if the same proteins control nitrile production from tryptophan-derived glucosinolates as from methionine-derived glucosinolates. In this report, we formally test if the proteins involved in controlling aliphatic glucosinolate hydrolysis during tissue disruption can control production of nitriles during indolic glucosinolate hydrolysis. We show that myrosinase is not sufficient for indol-3-acetonitrile production from indol-3-ylmethyl glucosinolate and requires the presence of functional epithospecifier protein *in planta* and *in vitro* to produce significant levels of indol-3-acetonitrile. This reaction is also controlled by the *Epithiospecifier modifier 1* gene. Thus, like formation of nitriles from aliphatic glucosinolates, indol-3-acetonitrile production following tissue disruption is controlled by multiple loci raising the potential for complex regulation and fine tuning of indol-3-acetonitrile production from indol-3-ylmethyl glucosinolate.

Keywords: *Arabidopsis thaliana*; Brassicaceae; Quantitative genetics; Biochemical assay; Indole glucosinolate; Indol-3-acetonitrile; Indol-3-carbinol; Epithiospecifier protein; Epithiospecifier modifier 1 protein

1. Introduction

Glucosinolates are sulfur-rich plant secondary metabolites whose basic skeleton consists of a β-thioglucose residue, an *N*-hydroxyiminosulfate moiety, and a variable side-chain. Generally, glucosinolates are grouped into aliphatic, aromatic and indole glucosinolates depending on whether they originate from aliphatic amino acids, aromatic amino acids, or tryptophan (Bones and Rossiter, 1996; Halkier and Du, 1997; Wittstock and Halkier 2002; Kliebenstein et al., 2001; Kliebenstein 2004; Kliebenstein et al., 2005; D'Auria and Gershenzon 2005). While the tryptophan-derived indole glucosinolates represent only five of the more than 120 known glucosinolate structures, they are present in a broad range of plants (Fahey et al., 2001). Indole glucosinolates are typically induced in response to insect herbivory and via the application of plant signaling molecules (Kliebenstein et al., 2002a; Mikkelsen et al., 2003). Additionally, they have been associated with cancer-promoting activity in the human diet (Fahey et al., 2001). Further, the breakdown products from indole glucosinolates have been identified as phytoalexins in various Brassica species, suggesting that they have a role in plant defense (Pedras et al., 2003, 2006).

* Corresponding author. Tel.: +1 530 754 7775; fax: +1 530 752 9659.
E-mail address: Kliebenstein@ucdavis.edu (D.J. Kliebenstein).
URL: www.plantsciences.ucdavis.edu/kliebenstein/ (D.J. Kliebenstein).

0031-9422/$ - see front matter © 2007 Elsevier Ltd. All rights reserved.
doi:10.1016/j.phytochem.2007.08.027

The predominant biological activities of glucosinolates are associated with their breakdown into various products by the action of the thioglucosidase, myrosinase, during tissue disruption (Halkier and Gershenzon, 2006; Kliebenstein et al., 2005). This can lead to the production of diverse activation structures including nitriles, isothiocyanates (ITC) and thiocyanates (Bones and Rossiter, 1996). Recent investigations have begun to show that the production of these different structures during the activation of methionine-derived glucosinolates is controlled by additional proteins (Burow et al., 2007; 2006b; Lambrix et al., 2001; Matusheski et al., 2006; Zhang et al., 2006). The epithiospecifier protein (ESP) has been shown to divert the methionine activation products towards nitriles or epithionitriles depending upon the glucosinolate structure (Burow et al., 2006a,b; Lambrix et al., 2001). In addition,

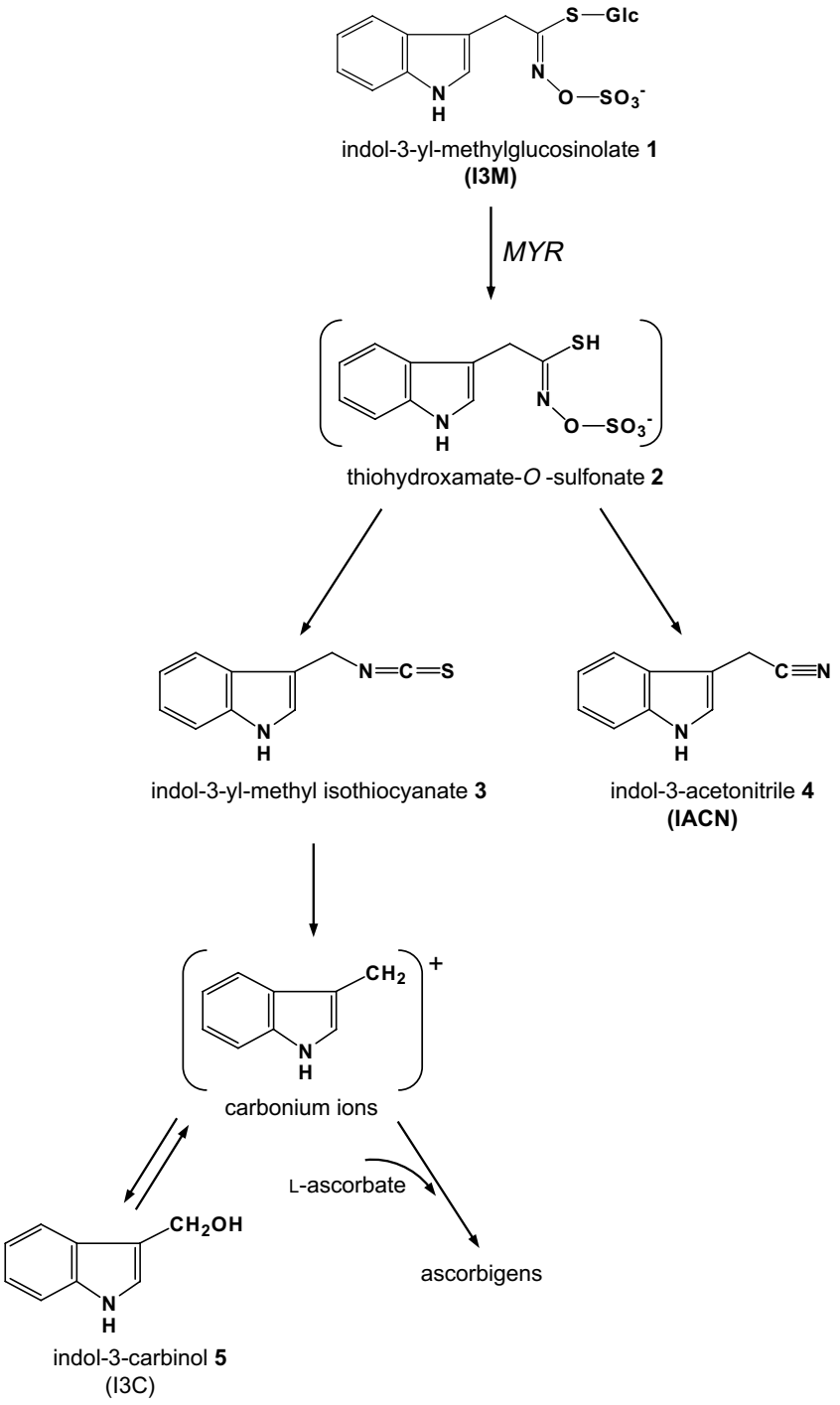

Fig. 1. Indole glucosinolate hydrolysis. Myrosinase-catalyzed hydrolysis of indole glucosinolates yields unstable aglycones as shown for indol-3-ylmethyl glucosinolate **1** which can give rise to several different metabolites depending on the reaction conditions. Spontaneous rearrangement leads to the corresponding isothiocyanate (3-(isothiocyanatomethyl)-1*H*-indole) formation followed by generation of indol-3-carbinol (I3C, [(1*H*-indol-3-yl)methanol]) **5** or ascorbigen. An alternative pathway leads to the generation of indol-3-acetonitrile (IACN, 2-[(1*H*-indol-3-yl)acetonitrile]) **4.** (*MYR*, myrosinase).

the ESP mediated nitrile formation can be inhibited by presence of the *ESM1* (*Epithiospecifier modifier 1*) gene leading to increased ITC production during glucosinolate activation (Burow et al., 2006b; Lambrix et al., 2001; Zhang et al., 2006). *ESM1* encodes a protein belonging to a known class of myrosinase-associated proteins.

While the above previous work has illuminated how methionine-derived glucosinolate activation is controlled, little is known about how tryptophan-derived glucosinolates are activated. In the absence of supplementary factors, the hydrolysis of indol-3-ylmethyl glucosinolate, I3M (**1**) by myrosinase leads to the production of the isothiocyanate **3** but not the nitrile **4** (Fig. 1) (Agerbirk et al., 1998; Chevolleau et al., 1997). The unstable indol-3-ylmethyl isothiocyanate **3** spontaneously and rapidly degrades to indol-3-carbinol (I3C) **5** which is then converted to ascorbigen in the presence of free ascorbate (Agerbirk et al., 1998; Chevolleau et al., 1997). In contrast, if the indol-3-ylmethyl glucosinolate **1** was converted into the nitrile, it would form indol-3-acetonitrile (IACN) **4** (Fig. 1).

While the conversion of indol-3-ylmethyl glucosinolate, to IACN **4** is known to occur (Agerbirk et al., 1998), it is currently unknown which factors in the plant favor the production of IACN **4** over I3C **5**. One potential mechanism is that myrosinase can produce IACN **4** from indol-3-yl-methyl glucosinolate **1** in the presence of free Fe^{2+}. However, the levels of free Fe^{2+} tested *in vitro* are likely not physiological levels (Agerbirk et al., 1998). Another possible source of IACN **4** could be the hydrolysis of indole glucosinolates in the presence of ESP. If *ESP* and *ESM1* also influence the hydrolysis of indole glucosinolates, this would enable a tight regulation of IACN **4** production *in planta*. Further, the relationship between IACN **4** produced during glucosinolate activation and the significant endogenous IACN **4** levels remains unknown (Ljung et al., 2005).

In this report, we show that both *ESP* and *ESM1* can control the production of nitriles from multiple indole glucosinolates in a quantitatively epistatic manner. Further, our data suggest that there are a number of additional genetic loci controlling the accumulation of IACN **4** in macerated tissue. This establishes a possible pathway by which IACN **4** may be generated during herbivore attack via the interaction of myrosinase and various associated proteins. Testing and understanding the relationship of IACN **4** produced during indole glucosinolate activation and other endogenous IACN **4** pools will further improve our understanding of this metabolite's role in plant defense.

2. Results

2.1. QTL for indole glucosinolate hydrolysis

To identify genetic loci controlling glucosinolate hydrolysis, we conducted an analysis of hydrolysis products of endogenous glucosinolates following tissue maceration in 54 L*er* × Col recombinant inbred lines (RIL) (Lambrix et al., 2001; Lister and Dean, 1993). The tissue maceration was designed to mimic tissue disruption as would, for example, occur during herbivory or mechanical wounding. We focused specifically on the production of IACN **4** to find the loci controlling nitrile production from indole glucosinolates. We were not able to reliably detect the I3C **5** product, presumably due to the low indole glucosinolate levels in these RILs and the rapid conversion of I3C **5** to ascorbigen (Agerbirk et al., 1998). We identified three QTL controlling IACN **4** accumulation. One locus corresponded to the previously identified *ESP* locus that contains the gene for ESP which has been shown to direct the production of simple nitriles from methionine-derived glucosinolates (Lambrix et al., 2001). Our results suggest that *ESP* also mediates the conversion of indole glucosinolates into their simple nitrile hydrolysis products. A second QTL, *ESM2*, at the top of chromosome I had been previously associated with myrosinase activity in this RIL population (Kliebenstein et al., 2002b; Mitchell-Olds and Pedersen, 1998). The third QTL, *ESM3*, at the bottom of chromosome *V* is associated with a QTL controlling the production of indole glucosinolates and may impact IACN **4** levels by controlling the accumulation of the indole glucosinolate precursors (Kliebenstein et al., 2002a, 2001) (Table 1). However, *ESM3* was found to epistatically interact with *ESP* with respect to the production of IACN **4** suggesting that it may function in the actual hydrolysis pathway rather than be simply causing an alteration in the level of intact indole glucosinolates (Table 1). Interestingly, the *ESM1* QTL that epistatically interacts with *ESP* to control the production of nitriles from methionine-derived glucosinolates was not statistically identified as impacting IACN production in this small subset of L*er* × Col RILs (Lambrix et al., 2001; Zhang et al., 2006).

2.2. ESP controls nitrile production during indole glucosinolate hydrolysis

The QTL analysis suggested that the *ESP* locus, previously known to control the production of nitriles during methionine-derived glucosinolate hydrolysis may also control nitrile production in the hydrolysis of indole glucosinolates (Table 1). To confirm this, we tested the effect of over-expression of *ESP* in the *ESP*-deficient Col-0 background upon the hydrolysis of endogenous indole glucosinolates. Lines expressing *ESP* under the control of the 35S promoter showed a dramatic increase in the production of IACN **4** during indole glucosinolate hydrolysis (Fig. 2). This was confirmed in three independent transgenic lines. Further, no changes in IACN **4** production were observed in control lines carrying the empty pPZP221 vector compared to the Col-0 wildtype. None of the lines showed elevated levels of intact indole glucosinolates in comparison to the Col-0 wildtype and the vector control lines (Burow et al., 2006b). This suggests that *ESP* mediates IACN **4** production during indol-3-yl-methyl

Table 1
QTL for IACN **4** Accumulation in 54 L*er* × Col RILs

QTL[a]	Chromosome[b]	Marker[c]	Position (cM)	LOD[d]	Effect[e]
ESM2	1	F21B7	8	4.1	5.3
ESP	1	nga280	86	20.0	−34.6
ESM3	5	nga151	21	18.1	−19.5
ESP × ESM3				15.3	13.2

QTL were mapped that control the accumulation of IACN **4** within 54 RILs from the L*er* × Col population. Composite interval mapping was used to identify the genetic loci.

[a] QTL shows the name of the QTL as well as any significant epistatic interactions.

[b] Chromosome shows the chromosome upon which the QTL is located.

[c] Marker lists the marker nearest to the QTL peak.

[d] LOD is the value of the test-statistic at the marker nearest to the QTL peak. The 0.05 significance threshold was 3.15 for this trait.

[e] Effect shows the percent phenotypic change caused by an allelic substitution at that QTL/Marker. Positive/Negative shows the directionality with regards to the Col-0 allele such that a positive number indicates that the Col-0 allele leads to higher accumulation of IACN **4** than the L*er* allele.

glucosinolate, **1** hydrolysis and that in the absence of functional ESP the major proportion of indole glucosinolates does not hydrolyze to IACN **4** (Fig. 2).

2.3. ESP directly mediates IACN production

We had previously shown that recombinant ESP was sufficient to direct myrosinase mediated hydrolysis of methionine-derived glucosinolates to either the simple nitrile or epithionitrile *in vitro* (Burow et al., 2006b; Lambrix et al., 2001; Zhang et al., 2006). Here, we incubated purified indole glucosinolates with purified myrosinase in the presence or absence of purified recombinant ESP. Myrosinase-catalyzed hydrolysis of indol-3-yl-methyl glucosinolate **1** in the absence of ESP lead solely to the production of the isothiocyanate-derived I3C, **5** and no IACN **4** was detected (Fig. 3). When purified recombinant ESP was added to the reaction, IACN **4** was detected in levels similar to I3C **5** (Fig. 3). Similar results were obtained when we used 4-methoxy- and *N*-methoxy-indol-3-yl-methyl glucosinolates (data not shown). Thus, myrosinase alone does not generate IACN **4** under the tested conditions. For IACN **4** production, an extra factor, ESP, is required. This is in agreement with previous observations about nitrile production from methionine-derived glucosinolates (Burow et al., 2006b; Lambrix et al., 2001).

2.4. ESM1 is a semi-dominant locus for indole glucosinolate hydrolysis

The RIL QTL analysis did not statistically identify *ESM1* as controlling indole glucosinolate hydrolysis. However, this population was small and may have lacked the statistical power to identify the phenotypic signal of variation at the *ESM1* locus. To specifically test if genetic variation at *ESM1* may control IACN **4** production, we assessed indole glucosinolate hydrolysis upon tissue maceration in two L*er* × Col-0 RIL's, CS1995 and CS1945, as well as in their reciprocal F_1 progeny. CS1995 and CS1945 are two RILs that are genetically identical at the three previously identified IACN QTLs and contain similar indole glucosinolate levels but genetically differ for the *ESM1* locus. We found that the *ESM1* region contains a QTL controlling indole glucosinolate hydrolysis in a semi-dominant manner (Fig. 4). The average IACN **4** production was 0.56, 0.65 and 0.81 μmol/g FW for CS1945, F_1 plants and CS1995, respectively, and the IACN **4** levels were significantly different from each other in a students *t*-test (Fig. 4). Analysis of indole glucosinolate hydrolysis products and genetic marker analysis of 190 F_2 individuals generated by selfing the F_1 of the CS1995 × CS1945 cross showed that the variation in indole glucosinolate hydrolysis between CS1995 and CS1945 could be treated as a single co-dominant Mendelian locus centred within 1 cM of the *ESM1* locus (by IACN accumulation: 43 plants $ESM1^{LerLer}$, 101 plants $ESM1^{LerCol}$ and 46 plants $ESM1^{ColCol}$, $\chi^2 = 0.853 < P_{0.05,2} = 5.991$). The semi-dominant nature of the *ESM1* QTL limits our ability to predict whether the functional allele is promoting or repressing nitrile formation.

2.5. ESP and ESM1 epistatically interact to control IACN

Previous work had shown that *ESP* and *ESM1* epistatically interact to control the hydrolysis of aliphatic glucosinolates (Lambrix et al., 2001; Zhang et al., 2006). This epistasis fits the quantitative genetics definition of epistasis which is non-additive for effects between loci (Lynch and Walsh, 1998; Lambrix et al., 2001; Mackay, 2001). To test for quantitative epistasis between *ESP* and *ESM1*, we genotyped the *ESP* and *ESM1* loci from 200 F_2 plants of a CS1945 × SALK-043148 (*ESM1* KO) cross. We then measured the IACN **4** levels following tissue disruption in 10 lines for each of the 9 different genotypic classes with respect to *ESP* and *ESM1* (Fig. 5). ANOVA with this data showed that there is a quantitative epistatic interaction between *ESP* and *ESM1* in controlling the production of IACN ($P = 0.004$ for the interaction term, $P < 0.001$ for the *ESP* and *ESM1* terms separately). This epistasis fits the quantitative genetics definition of epistasis in that it is a non-additive interaction of alleles at both loci

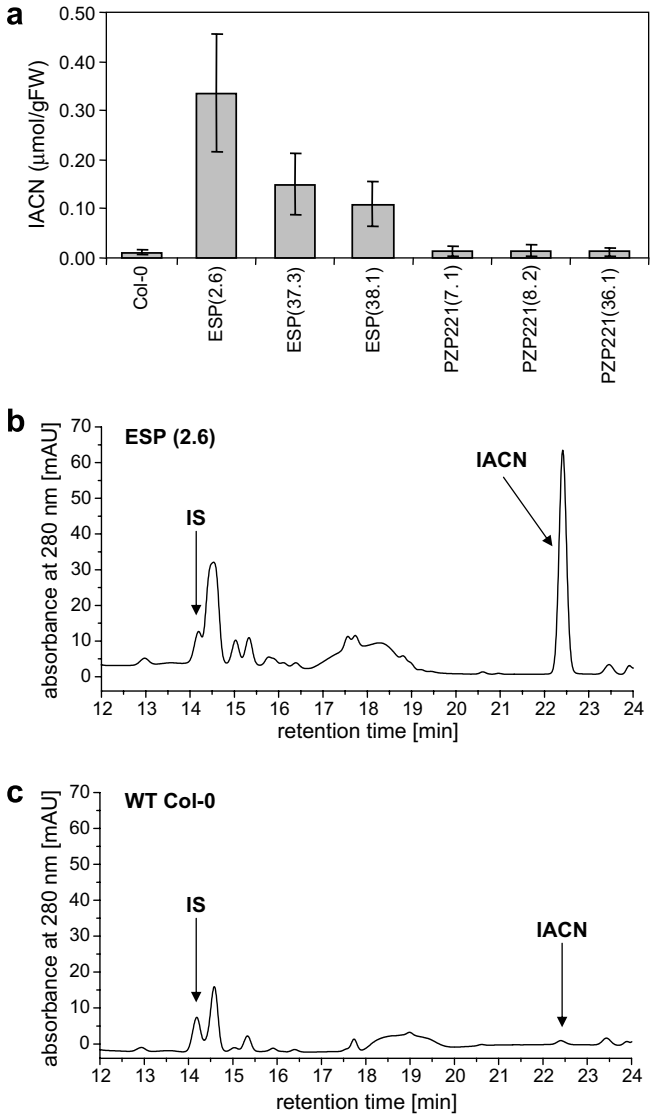

Fig. 2. *ESP* over-expression increases *in planta* formation of IACN upon tissue disruption. IACN levels were determined by HPLC of aqueous extracts of rosette leaves of WT Col-0, three independent homozygous transgenic lines (T_4) over-expressing ESP (ESP 2.6, 37.3 and 38.1) and three independent homozygous transgenic lines (T_4) transformed with the empty vector as a negative control (PZP221 7.1, 8.2 and 36.1). (a) IACN **4** levels. Eight to eleven plants per line were tested in three independent experiments. Given values are means ± standard deviations. (b) Representative HPLC trace from a T_4 line over-expressing ESP (2.6). (c) Representative HPLC trace from WT Col-0.

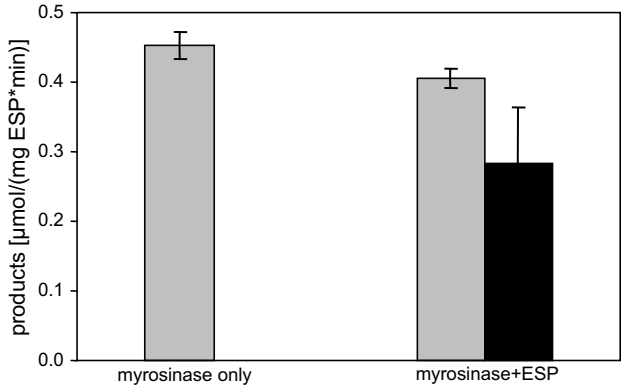

Fig. 3. Purified ESP directs IACN formation *in vitro*. Indol-3-yl-methyl glucosinolate **1** was incubated with either purified myrosinase or purified myrosinase plus purified recombinant ESP. The rates of formation of indol-3-carbinol (I3C, grey) **5** and indol-3-acetonitrile (IACN, black) **4** are shown. The assays were done in triplicate.

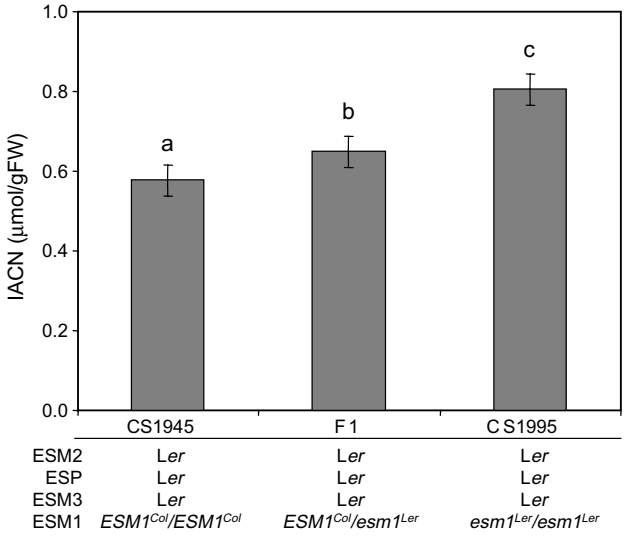

Fig. 4. *ESM1* controls IACN formation. Shown is the IACN **4** level following tissue maceration of two RILs (CS1945 and CS1995) and their resulting F_1. The genotype at the three detected IACN QTL is listed below the graph. The genotype at the *ESM1* locus is also shown with large letters for the functional allele and small letters for the knockdown allele. The genotypes were independently verified within the lab using markers near the QTL peak. The given values are means and standard errors from ten fold replication in two independent experiments. Letters above the bars show statistically different groups as determined by pairwise *t*-tests.

instead of the Mendelian definition of epistasis where an allele at one locus hides the variation at the second locus. The maximal IACN **4** production observed in the CS1945 × SALK-043148 (*ESM1* KO) F_2 is less than that for CS1995 where *ESP* and *ESM1* are both the L*er* allele (Figs. 4 versus 5). This is likely due to the low IACN Col-0 allele at the *ESM3* locus in this cross which originates from the *ESM1* KO. Additionally, the use of F_2 lines diminishes our power to separate means between the nine specific genotypic classes due to increased variation but increases our power to query the interaction between the loci.

2.6. The ESM1 gene controls structural specificity in hydrolysis of indole glucosinolates

We have previously identified the gene encoding a myrosinase-associated protein, At3g14210, as the gene underlying the *ESM1* QTL for nitrile production from methionine-derived glucosinolates. *ESM1* is highly expressed in Col-0 while lowly expressed in L*er* (Zhang et al., 2006). We used transgenic analysis to test if At3g14210 also controls IACN **4** production from indole glucosinolates. A T-DNA knockout of At3g14210/*ESM1* showed a 4-fold increase in the pro-

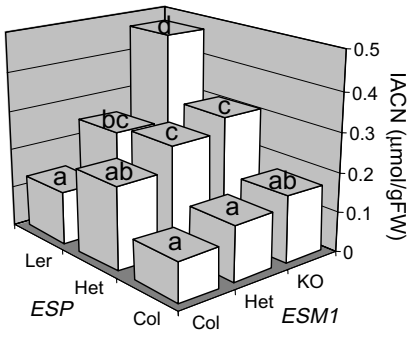

Fig. 5. Quantitative epistasis between *ESP* and *ESM1*. IACN **4** levels upon tissue disruption in 90 F_2 progeny, ten for each genotypic class, of the CS1945 × SALK-043148. The genotypes at the *ESP* and *ESM1* loci are shown on the *X* and *Y* axes, respectively. KO represents the *ESM1* KO allele obtained from SALK-043148. Letters within the top of each bar show genetic groupings that are statistically different as determined via F-tests within ANOVA. Shown are means from the ten replicates for each genotypic class. Standard errors for the nine genotypic classes ranged from 0.03 to 0.04 μmol/g FW.

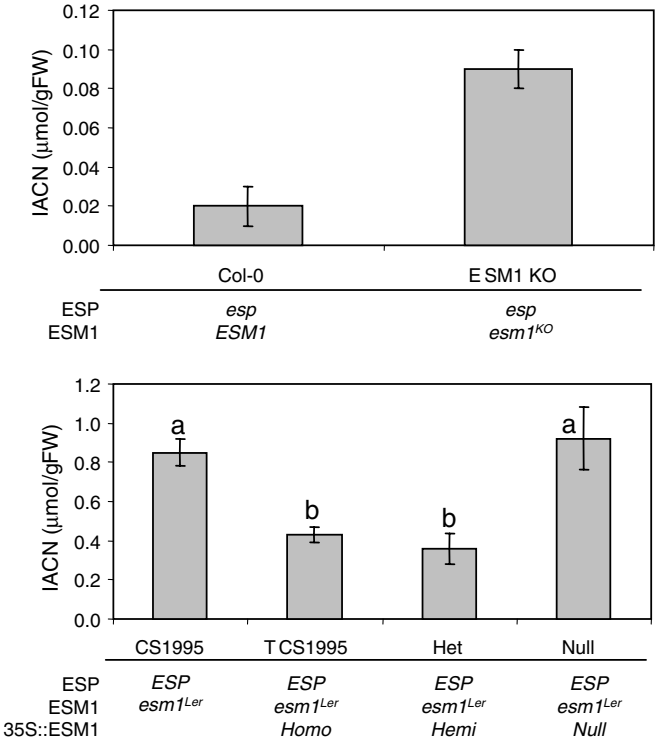

Fig. 6. *ESM1* controls *in planta* IACN accumulation. IACN **4** levels following tissue maceration in WT Col-0 and a homozygous T-DNA knockout in the *ESM1* gene (a) and RIL CS1995 and the TCS1995 transgenic line with 35S promoter driven *ESM1* expression (b) as determined by HPLC. The genotypes of *ESP* and *ESM1* are listed below the graphs. Additionally, the allele dosage of the 35S over-expression line is listed in (b) with Null referring to the segregants not containing any transgene. Given values are means and standard errors from five replicates in two independent experiments (a) and from five replicates of each of three independent lines per genotype with a single T-DNA-insertion tested in duplicate experiments (b). There were no significant differences between the independent transgenic lines of one genotype in (b).

duction of IACN **4** during indole glucosinolate hydrolysis in comparison to the Col-0 wildtype (Fig. 6a). The Col-0 accession contains a natural knockout of the *ESP* gene. Further, Col-0 and the *ESM1* T-DNA knockout line did not differ in their level of intact indole glucosinolates suggesting that the difference in IACN **4** formation is due to an altered structural outcome of glucosinolate hydrolysis. Because the lack of functional *ESM1* increases IACN **4** production, this suggests that *ESM1* functions to block/inhibit the production of IACN **4**.

To independently test *ESM1's* putative function, we transformed both CS1995 and CS1945 with an over-expression construct containing a 35S promoter in front of *ESM1*. CS1995 contains functional *ESP* and the low expression allele of *ESM1* while CS1945 contains functional *ESP* with the high expression allele of *ESM1* (Fig. 4) (Zhang et al., 2006). Analysis of indole glucosinolate hydrolysis products showed that over-expression of *ESM1* had a significant effect upon IACN **4** production in the CS1995 background where the endogenous *ESM1* was a low-expression allele (Fig. 6b). Over-expression of *ESM1* in CS1945, which contains the higher expressed *ESM1* allele, still caused a 30% decrease in IACN production that was statistically significant by *t*-test (data not shown). This agrees with the proposed function of *ESM1* being to repress/inhibit nitrile production, even in the presence of the *ESP* promoting nitrile formation.

3. Conclusions

3.1. ESP promotes IACN 4 formation during tissue disruption

Natural genetic variation, analysis of transgenic plants and recombinant protein *in vitro* showed that ESP is critical for the production of IACN **4** from indol-3-yl-methyl glucosinolate **1** in Arabidopsis rosette tissue. The natural knockdown allele of ESP present in the Col-0 accession led to a 90% reduction in the production of IACN **4** *in planta* as compared to L*er* (Fig. 2). Furthermore, the introduction of purified ESP into a mixture of indol-3-yl-methyl glucosinolate **1** and purified myrosinase led to the production of IACN **4**, whereas purified myrosinase alone was unable to generate IACN **4** (Fig. 3). Thus, ESP is a critical component of IACN **4** production during tissue disruption of Arabidopsis rosette leaves.

3.2. ESM1 inhibits IACN 4 formation during tissue disruption

Natural genetic variation and indole glucosinolate hydrolysis in transgenic lines showed that *ESM1* also controls *in planta* production of IACN **4** from indol-3-yl-methyl glucosinolate **1** (Fig. 4). However, in analogy to its role in the hydrolysis of methionine-derived glucosinolates (Zhang et al., 2006), active *ESM1* appears to inhibit

the formation of IACN **4** from indol-3yl-methyl glucosinolate **1** following tissue disruption (Fig. 6). Thus, the generation of IACN **4** during indol-3-yl-methyl glucosinolate **1** hydrolysis is dependent on a complex interaction involving at least *ESM1*, *ESP* and myrosinase.

3.3. Competitive control of IACN formation

The counteracting roles that *ESP* and *ESM1* play in either causing or inhibiting nitrile production from indole glucosinolates set up a unique regulatory system to fine-tune the level of nitrile versus isothiocyanate production (Fig. 1). The plant may determine the outcome of glucosinolate hydrolysis by regulating the expression of the *ESP*, *ESM1* and further, so far unknown genes. This concept is already supported by studies showing that naturally variable gene expression of *ESP* and *ESM1* plays a role in determining the structural specificity of glucosinolate hydrolysis in the different Arabidopsis accessions (Kliebenstein et al., 2006; Lambrix et al., 2001; Zhang et al., 2006). It will be interesting to see if the plant uses various signals, jasmonate, salicylate, ethylene, auxin, etc., to modulate the relative expression of *ESP* and *ESM1* to make glucosinolate hydrolysis responsive to the environment. The non-additivity of the *ESP* and *ESM1* interaction shows that even if the transcripts of both genes are co-ordinately induced, the outcome of the hydrolysis will change (Fig. 5). In combination with the second QTL identified (which has not been cloned so far) this sets up myrosinase-catalyzed glucosinolate hydrolysis as a complex biochemical mechanism by which the ratio of nitrile versus isothiocyanate products obtained may be finely tuned by regulation of several proteins.

3.4. IACN *4* versus I3C *5* in plant defense

Glucosinolate activation/hydrolysis occurs during tissue disruption typically associated with a herbivore. This leads to the production of glucosinolate activation products both in the tissue being ingested by the herbivore as well as in the residual disrupted tissue that was not eaten. Variation within glucosinolate activation products in the ingested tissue are believed to control genetic variation in herbivore resistance (Barth and Jander, 2006; Burow et al., 2006a; Jander et al., 2001; Lambrix et al., 2001; Zhang et al., 2006). However, the presence of glucosinolate activation products in the disrupted tissue that was not eaten may also have a function. It is possible that the remaining activation products could provide anti-microbial activity that would potentially sterilize any cut site (Pedras et al., 2003, 2006). Additionally, in the case of indole glucosinolates, this might yield a pool of indole-acetonitriles **4** that could be utilized by the plant to make plant defensive compounds at the site of disruption. The relative roles of IACN **4** versus I3C **5** as obtained from indol-3-yl-methyl glucosinolate **1** activation remain to be shown. This work provides the genetic tools necessary to modulate the production of these activation products to allow for direct tests of their functions.

3.5. Future work

This work shows that, following tissue disruption, IACN **4** can be generated from indole glucosinolates through the action of ESP and myrosinase, and that its production is regulated by *ESM1*. Future work will have to focus on the roles of the methylated versions of indole glucosinolates and their corresponding nitriles and carbinols. Further, is the main role of indole glucosinolate activation products within the herbivore or is it to produce a pool of IACN **4** or I3C **5** in the tissue left behind which can then possibly be utilized to produce other metabolites or function directly as phytoalexins within the plant (Pedras et al., 2003, 2006)? Additional work will also be required to test if *ESP*, *ESM1*, myrosinase or their homologues provide any IACN **4** in the absence of tissue hydrolysis. This work should better clarify what if any role indole glucosinolate activation plays in plant defense.

4. Experimental

4.1. QTL analysis

Fifty-four L*er* × Col recombinant inbred lines (RIL) were grown and analyzed for glucosinolate hydrolysis product formation after tissue maceration in water as previously described (Lambrix et al., 2001). The phenotypic data were then used for QTL mapping by means of the multiple-interval mapping algorithm of the QTL Cartographer package as previously described (Basten et al., 1999; Denby et al., 2004; Zeng et al., 1999).

4.2. Plant material for ESP analysis

Transgenic lines of *A. thaliana* Col-0, which express the *ESP* cDNA from *A. thaliana* L*er* under the control of the CaMV35S promoter, were generated and characterized as described (Burow et al., 2006b). Independent lines with a single T-DNA insertion were selected according to the segregation of the selection marker (T_3 generation). Plants used in the experiments were grown on soil in a controlled climate chamber (21 °C, 55% relative humidity, and 100 μmol m^{-2} s^{-1} photosynthetically active radiation) for 4 weeks. The photoperiod was 10-h light, 14-h dark.

4.3. Plant growth for ESM1 analysis

All plants for *ESM1* analysis were grown in a Conviron growth chamber under 20 °C, 60% relative humidity, using a photoperiod of 16 h light and 8 h dark with white fluorescent lights at 100 μEi m^{-2} s^{-1} photosynthetically active radiation. Transgenic lines either containing a T-DNA insertion in the *ESM1* locus or, which express the *ESP*

cDNA from *A. thaliana* Col-0 under the control of the CaMV35S promoter, were generated and characterized as previously described (Zhang et al., 2006). Independent lines with a single T-DNA insertion were selected according to the segregation of the selection marker (T_3 generation). Flats with 104 cells were used for planting with a single plant per cell generating a density of 1040 plants m^{-2}. General purpose growing medium PREMIER PRO-MIX soil with slow release osmocote fertilizer was used.

4.4. Glucosinolate substrates and hydrolysis product standards

Indole glucosinolates were isolated from seeds of *Isatis tinctoria* as described (Thies, 1988) with the modification that the indole glucosinolates were eluted from the DEAE Sephadex with the application of an additional 75 mL of 0.5 M potassium sulfate. Individual indole glucosinolates were separated and fractionated by HPLC (Mellon et al., 2002). 1-isothiocyanato-propane (propyl isothiocyanate) and (1*H*-indol-3-yl)-methanol (indol-3-carbinol, I3C) **5** were purchased from Sigma–Aldrich; 3-(2-hydroxyethyl)indole was from Fluka; (1*H*-indol-3-yl)-acetonitrile, IACN, **4** was from Riedel de Haen.

4.5. HPLC of glucosinolate hydrolysis products

Hydrolysis products from indole glucosinolates were separated by HPLC on an Agilent HP1100 Series instrument equipped with a C-18 reversed phase column (LiChrospher RP18ec, 250 × 4.6 mm, 5 μm particle size) using a H_2O (solvent A)-CH_3CN (solvent B) gradient at a flow rate of 1 ml min^{-1} at 25°C. The injection volume was 50 μL. For plant extracts, the gradient was 15–42% B (27 min), 42–100% B (0.5 min), a 2-min hold at 100% B, 100–15% B (0.5 min), and a 5-min hold at 15% B. For ESP assays, a gradient of 15–75% B (15 min), 75–100% B (5 min), a 2-min hold at 100% B, 100–15% B (0.1 min), and a 4.9-min hold at 15% B was used. Eluents were monitored by diode array detection between 190 and 360 nm (2 nm interval). (1*H*-indol-3-yl)-acetonitrile **4** and (1*H*-indol-3-yl)-methanol were identified by comparison of the retention times and UV spectra with those of standards.

4.6. Analysis of glucosinolate hydrolysis products in plant extracts

Crude protein extracts (100 mg) were prepared from rosette leaves of *A. thaliana* by grinding leaf material with 300 μL of 50 mM MES, pH 6.0, followed by incubation at room temperature for 5 min. 10 μL of 3-(2-hydroxyethyl)indole (1 mM in CH_3CN) were added as an internal standard. After centrifugation at 10,000*g* for 10 min, CH_3CN (300 μl) were added to the supernatant. Insoluble material was removed by centrifugation at 10,000*g* for 3 min. Samples were analyzed by HPLC. (1*H*-indol-3-μl)-CH_3CN (IACN) **4** was quantified based on the peak area at 280 nm relative to the peak area of the internal standard (relative response factor 1.0).

4.7. Analysis of ESP activity in vitro

The ESP cDNA (L*er*) was cloned into the pCRT7/CT-TOPO expression vector (Invitrogen) and expressed in *E. coli* BL21(DE3)pLysS (Invitrogen) with an N-terminal *Strep*-tag II (IBA GmbH, Göttingen, Germany). The recombinant protein was purified from the bacterial extract by Strep-Tactin affinity chromatography (IBA GmbH, Göttingen, Germany) (Burow et al., 2006b). ESP assays were done in a total volume of 500 μl 50 mM MES buffer, pH 6.0, with 8 μg ESP. Indol-3-yl-methylglucosinolate **1** and 1-methoxy-indol-3-yl-methylglucosinolate were added to the assay mixture to a final concentration of 0.85 mM and 0.5 mM, respectively. The reaction was started by addition of 50 ng myrosinase purified from seeds of *Sinapis alba* (Burow et al., 2006b). After incubation at room temperature (22–24 °C) for 1 h, 40 μl of propyl isothiocyanate (1.13 μg/μl in methanol) were added as internal standard. Samples were separated by HPLC and (1*H*-indol-3-yl)-acetonitrile (IACN) **4** and (1*H*-indol-3-yl)-methanol (I3C) **5** were quantified based on the peak area at 240 nm relative to the peak area of the internal standard using relative response factors as described by Matthaeus (Matthaeus and Fiebig, 1996).

Acknowledgements

Michael Reichelt is thanked for providing purified indole glucosinolate substrates. This project was funded by The Max Planck Society and NSF MCB 0323759 and NSF DBI 0642481 awarded to DJK.

References

Agerbirk, N., Olsen, C.E., Sorensen, H., 1998. Initial and final products, nitriles, and ascorbigens produced in myrosinase-catalyzed hydrolysis of indole glucosinolates. J. Agri. Food Chem. 46, 1563–1571.

Barth, C., Jander, G., 2006. Arabidopsis myrosinases TGG1 and TGG2 have redundant function in glucosinolate breakdown and insect defense. Plant J. 46, 549–562.

Basten, C.J., Weir, B.S., Zeng, Z.-B., 1999. QTL Cartographer, Version 1.13. Department of Statistics, North Carolina State University, Raleigh, N.C.

Bones, A.M., Rossiter, J.T., 1996. The myrosinase-glucosinolate system, its organisation and biochemistry. Phys. Plant. 97, 194–208.

Burow, M., Bergner, A., Gershenzon, J., Wittstock, U., 2007. Glucosinolate hydrolysis in *Lepidium sativum* – identification of the thiocyanate-forming protein. Plant Mol. Biol. 63, 49–61.

Burow, M., Markert, J., Gershenzon, J., Wittstock, U., 2006a. Comparative biochemical characterization of nitrile-forming proteins from plants and insects that alter myrosinase-catalysed hydrolysis of glucosinolates. FEBS J. 273, 2432–2446.

Burow, M., Muller, R., Gershenzon, J., Wittstock, U., 2006b. Altered glucosinolate hydrolysis in genetically engineered *Arabidopsis thaliana* and its influence on the larval development of *Spodoptera littoralis*. J. Chem. Ecol. 32, 2333–2349.

Chevolleau, S., Gasc, N., Rollin, P., Tulliez, J., 1997. Enzymatic, chemical, and thermal breakdown of H-3-labeled glucobrassicin, the parent indole glucosinolate. J. Agri. Food Chem. 45, 4290–4296.

D'Auria, J.C., Gershenzon, J., 2005. The secondary metabolism of *Arabidopsis thaliana*: growing like a weed. Curr. Opin. Plant Biol. 8, 308–316.

Denby, K.J., Kumar, P., Kliebenstein, D.J., 2004. Identification of *Botrytis cinerea* susceptibility loci in *Arabidopsis thaliana*. Plant J. 38, 473–486.

Fahey, J.W., Zalcmann, A.T., Talalay, P., 2001. The chemical diversity and distribution of glucosinolates and isothiocyanates among plants. Phytochemistry 56, 5–51.

Halkier, B.A., Du, L., 1997. The biosynthesis of glucosinolates. Trends Plant Sci. 2, 425–431.

Halkier, B.A., Gershenzon, J., 2006. Biology and biochemistry of glucosinolates. Ann. Rev. Plant Biol. 57, 303–333.

Jander, G., Cui, J., Nhan, B., Pierce, N.E., Ausubel, F.M., 2001. The TASTY locus on chromosome 1 of Arabidopsis affects feeding of the insect herbivore *Trichoplusia ni*. Plant Physiol. 126, 890–898.

Kliebenstein, D.J., 2004. Secondary metabolites and plant/environment interactions: a view through *Arabidopsis thaliana* tinged glasses. Plant Cell Environ. 27, 675–684.

Kliebenstein, D.J., Figuth, A., Mitchell-Olds, T., 2002a. Genetic architecture of plastic methyl jasmonate responses in *Arabidopsis thaliana*. Genetics 161, 1685–1696.

Kliebenstein, D.J., Gershenzon, J., Mitchell-Olds, T., 2001. Comparative quantitative trait loci mapping of aliphatic, indolic and benzylic glucosinolate production in *Arabidopsis thaliana* leaves and seeds. Genetics 159, 359–370.

Kliebenstein, D.J., Kroymann, J., Mitchell-Olds, T., 2005. The glucosinolate-myrosinase system in an ecological and evolutionary context. Curr. Opinion Plant Biol. 8, 264–271.

Kliebenstein, D.J., Pedersen, D., Mitchell-Olds, T., 2002b. Comparative analysis of insect resistance QTL and QTL controlling the myrosinase/glucosinolate system in *Arabidopsis thaliana*. Genetics 161, 325–332.

Kliebenstein, D.J., West, M.A.L., Van Leeuwen, H., Kyunga, K., Doerge, R.W., Michelmore, R.W., St.Clair, D.A., 2006. Genomic survey of gene expression diversity in *Arabidopsis thaliana* Genetics 10.1534/genetics.105.049353.

Lambrix, V., Reichelt, M., Mitchell-Olds, T., Kliebenstein, D., Gershenzon, J., 2001. The Arabidopsis epithiospecifier protein promotes the hydrolysis of glucosinolates to nitriles and influences *Trichoplusia ni* herbivory. Plant Cell 13, 2793–2807.

Lister, C., Dean, D., 1993. Recombinant inbred lines for mapping RFLP and phenotypic markers in *Arabidopsis thaliana*. Plant J. 4, 745–750.

Ljung, K., Hull, A.K., Celenza, J., Yamada, M., Estelle, M., Nonmanly, J., Sandberg, G., 2005. Sites and regulation of auxin biosynthesis in Arabidopsis roots. Plant Cell 17, 1090–1104.

Lynch, M., Walsh, B., 1998. Genetics and analysis of quantitative traits. Sinauer Associates, Inc., Sunderland, Massachusetts.

Mackay, T.F.C., 2001. The genetic architecture of quantitative traits. Annu. Rev. Genet. 35, 303–339.

Matthaeus, B., Fiebig, H.J., 1996. Simultaneous determination of isothiocyanates, indoles, and oxazolidinethiones in myrosinase digests of rapeseeds and rapeseed meal by HPLC. J. Agri. Food Chem. 44, 3894–3899.

Matusheski, N.V., Swarup, R., Juvik, J.A., Mithen, R., Bennett, M., Jeffery, E.H., 2006. Epithiospecifier protein from broccoli (*Brassica oleracea* L. ssp. *italica*) inhibits formation of the anticancer agent sulforaphane. J. Agri. Food Chem. 54, 2069–2076.

Mellon, F.A., Bennett, R.N., Holst, B., Williamson, G., 2002. Intact glucosinolate analysis in plant extracts by programmed cone voltage electrospray LC/MS: Performance and comparison with LC/MS/MS methods. Anal. Biochem. 306, 83–91.

Mikkelsen, M.D., Petersen, B.L., Glawischnig, E., Jensen, A.B., Andreasson, E., Halkier, B.A., 2003. Modulation of CYP79 genes and glucosinolate profiles in *Arabidopsis* by defense signaling pathways. Plant Physiol. 131, 298–308.

Mitchell-Olds, T., Pedersen, D., 1998. The molecular basis of quantitative genetic variation in central and secondary metabolism in *Arabidopsis*. Genetics 149, 739–747.

Pedras, M.S.C., Chumala, P.B., Suchy, M., 2003. Phytoalexins from *Thlaspi arvense*, a wild crucifer resistant to virulent *Leptosphaeria maculans*: structures, synthesis and antifungal activity. Phytochemistry 64, 949–956.

Pedras, M.S.C., Sarwar, M.G., Suchy, M., Adio, A.M., 2006. The phytoalexins from cauliflower, caulilexins A, B and C: Isolation, structure determination, synthesis and antifungal activity. Phytochemistry 67, 1503–1509.

Thies, W., 1988. Isolation of sinigrin and glucotropaeolin from Cruciferous seeds. Fat Sci. Technology 8, 311–314.

Wittstock, U., Halkier, B.A., 2002. Glucosinolate research in the Arabidopsis era. Trends Plant Sci. 7, 263–270.

Zeng, Z.-B., Kao, C.-H., Basten, C.J., 1999. Estimating the genetic architecture of quantitative traits. Gene. Res. 75, 345–355.

Zhang, Z.-Y., Ober, J.A., Kliebenstein, D.J., 2006. The gene controlling the quantitative trait locus *Epithiospecifier modifier 1* alters glucosinolate hydrolysis and insect resistance in Arabidopsis. Plant Cell 18, 1524–1536.